A Laser-Accelerator Injector Based on Laser Ionization and Ponderomotive Acceleration of Electrons

C. I. Moore, A. Ting, S. J. McNaught,* J. Qiu, H. R. Burris, and P. Sprangle

Beam Physics Branch, Plasma Physics Division, Naval Research Laboratory, Washington, D.C. 20375

(Received 15 October 1998)

A new laser-accelerator injector based on the high-energy electrons ejected from a laser focus following the ionization of high-charge states of gases has been investigated. This method can generate electron pulses with MeV energies and pulse widths substantially less than the laser pulse width using terawatt lasers. Experiments at intensities of 3×10^{18} W/cm^2 show that two highly directional electron beams with energies up to 340 keV are produced in the laser polarization direction. These highly directional beams are inconsistent with simulation results using Ammosov-Delone-Krainov (ADK) tunneling theory to model the ionization process. It is shown that this is likely due to the release of electrons with larger canonical momentum than predicted by ADK theory. [S0031-9007(99)08533-6]

Significant progress has been made on laser-based particle acceleration [1] in the past decade: Background plasma electrons have been accelerated to approximately 100 MeV [2]; extended focused propagation distances have been generated [3]; acceleration in plasma [2,4]; vacuum [5], and structures [6] has been observed; and clean sinusoidal accelerating plasma waves have been measured [7]. Despite these advances, many challenges remain. One of these challenges is a suitable electron injector. An ideal laser accelerator injector should satisfy the following requirements: (a) electron bunch lengths much less than the period of the accelerating field, (b) femtosecond timing between the injector pulse and the accelerating structure, (c) simplicity of operation and reasonable tolerance on alignment, and (d) a good emittance source. This injector will allow efficient coupling of the injector to the accelerator, and precise reproducible phasing and uniform acceleration of the electrons in the accelerating buckets.

Recently the LILAC [8] and the colliding pulse laser injector [9] schemes have been proposed. These concepts are attractive since they are predicted to produce small emittance electron pulses a few femtoseconds long with excellent synchronization between the injector and accelerator. However, they require extremely tight tolerances on alignment and are unsuitable for nonplasma-based accelerators.

We have performed experimental and numerical studies to investigate a new injector based on laser ionization and ponderomotive acceleration (LIPA) of electrons as an electron source. This scheme uses the electrons ejected from a high-intensity laser focus following ionization of high-charge states of gases [10,11] as an electron source. These electrons are ejected due to a combination of ponderomotive acceleration [12] and conservation of canonical momentum [13]. By appropriately choosing the gas, laser polarization, focusing geometry, and intensity, very short pulse electron bunches ($t \sim 5$ fs) with high energy ($E \sim 2.8$ MeV) and small emittance ($\varepsilon \sim 0.8$ mm · mrad) are achievable with current laser systems. In the preliminary experiments described here, we have observed well-directed electron beams with energies up to 340 keV.

The experiment used a linearly polarized 2.5 TW, 400 fs laser pulse from the NRL T^3 laser system ($\lambda = 1.054$ μm) focused to a peak intensity of 3×10^{18} W/cm^2 in a vacuum chamber backfilled with 1 Torr of krypton gas. Ejected electrons were measured by wrapping direct exposure x-ray film (DEF) in a 3-cm-diameter cylinder around the laser focus with the laser axis concomitant with the axis of the cylinder of film. Electrons exposed the film allowing measurement of the ejected electrons' angular distribution. One or three layers of 6 μm thick aluminum foil covered the film to prevent exposure from stray light and low-energy electrons.

Thomson scattered light at 1054 nm was imaged through an interference filter onto a charge-coupled device at 90° to the laser axis to determine the effects of atomic self-focusing (ASF) and ionization induced defocusing (IID) [14]. At background pressures of 10 Torr and below, no evidence for ASF or IID was observed—diffraction limited propagation was observed. At higher pressures, both IID (at 15 Torr and above) and ASF (at 50 Torr and above) were evident.

Figure 1 shows the observed electron distributions. Both images show the film "unrolled" with the horizontal axis as the azimuthal angle ϕ around the laser axis and the vertical axis as the z position along the laser axis (the focus is at $z = 0$). The small marks at $z = -3$ mm and $\phi = 90°$ are punch marks for locating the laser focus position. The polarization direction was in the $\phi = 90°$ and $\phi = 270°$ directions. Figure 1(a) shows the higher energy electron distribution, where three layers of aluminum foil completely blocked electrons below about 70 keV and significantly attenuated electrons up to approximately 140 keV [15]. For this image, nine laser shots were taken to expose the film with an optimal contrast. Figure 1(b) shows the lower energy electron component, where one
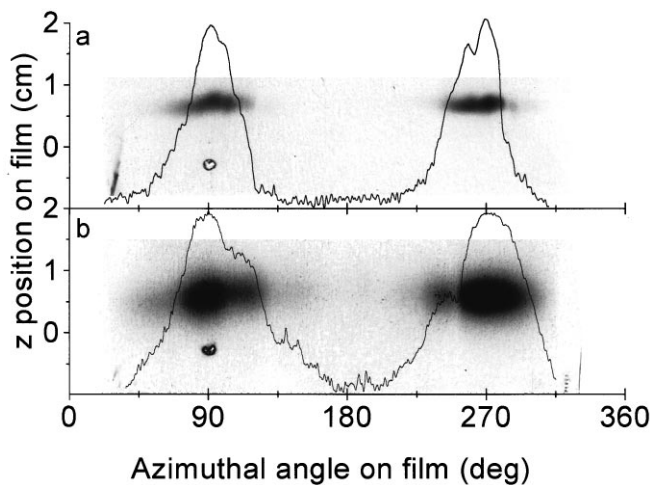
FIG. 1. Measured ejected electron distribution from LIPA on DEF x-ray film. (a) The distribution with three layers of aluminum foil covering the film ($E > 70$ keV). (b) The distribution with one layer of aluminum foil covering the film ($E > 35$ keV). The overlayed plots are lineouts showing the azimuthal intensity distribution.

layer of aluminum foil completely blocked about 35 keV electrons and significantly attenuated up to about 70 keV electrons [15]. For this image, four laser shots were taken.

Figures 1(a) and 1(b) show two highly directional electron "beams" oriented along the laser polarization direction (90° rotation of the polarization showed a corresponding rotation of the electron beams). Also apparent is the positive z positions of the beams due to a forward momentum component. Theory [16] and experiment [10] show that an ionized electron's ejection cone angle θ relative to the laser axis is related to its ejection energy by $\tan \theta = \sqrt{2/(\gamma - 1)}$, where γ is the relativistic factor of the electron. The electrons in Fig. 1(a) were ejected with cone angles ranging from $60° \pm 3°$ to $71° \pm 3°$ corresponding to electrons ejected with energies ranging from 120 ± 50 to 340 ± 90 keV. The uncertainties in angle and energy arise from a maximum uncertainty in the focal position relative to the film position of ± 1 mm. In Fig. 1(b), the thinner aluminum filtering allowed lower energy electrons to strike the film in addition to the high energy electrons observed in Fig. 1(a). The minimum cone angle of $60° \pm 3°$ and the corresponding energy of 340 ± 90 keV were the same in both Figs. 1(a) and 1(b); however, the maximum cone angle of $80° \pm 3°$ in Fig. 1(b) was much larger and the associated ejection energy of 32 ± 15 keV was much smaller. The appearance of only larger cone angle electrons as the aluminum thickness decreased clearly demonstrates the energy dependent ejection angle of LIPA. This suggests a simple energy selection method for LIPA which uses an "angle selector" to select electrons with cone angles corresponding to the energy range of interest.

Laser ionization and ponderomotive acceleration are driven by the single particle behavior of an electron ionized from an inner shell of an atom into an intense electromagnetic field. Laser ionization of electrons with orbital frequencies much greater than the field frequency occurs in the tunneling ionization regime [17,18]. The most accurate tunneling ionization theory, based on agreement with experiments, is the Ammosov-Delone-Krainov (ADK) tunneling theory [18]. Once free from the atom, electrons oscillate in the laser field with an average "ponderomotive" quiver energy of $\Phi_p[\text{eV}] = 9.33 \times 10^{-14} I[\text{W/cm}^2]\lambda^2[\mu\text{m}]$, where I is the laser intensity at the time of ionization and λ is the laser wavelength. In a spatially varying field, this ponderomotive quiver energy is converted to directed translational energy through the polarization independent ponderomotive force, $\vec{\text{F}}_p \propto -\vec{\nabla}\Phi_p$ [12]. For an azimuthally symmetric Gaussian laser focus, the ponderomotive force causes azimuthally symmetric ejection of electrons from the laser focus. For laser pulse lengths much greater than the electron ejection time from the focus, the ponderomotive energy is conserved resulting in ejection with the full ponderomotive energy. This is the case for our experiment, where the laser pulse length (400 fs) is approximately 10 times greater than the electron ejection times ($\sim$50 fs).

A strong field approximation for tunneling ionization is given by the barrier suppression ionization (BSI) model of ionization [19]. The BSI threshold intensity in a linearly polarized laser field is given by $I_{\text{th}}[\text{W/cm}^2] = 4 \times 10^9 E^4[\text{eV}]/Z^2$, where E is the electron binding energy and Z is the ionic charge. The BSI model does not accurately model all aspects of ionization (such as phase dependence), but has been shown to accurately predict the ionization threshold intensities observed in short pulse laser experiments [19]. From the BSI threshold intensity, we can estimate that up to Kr^{18+} ($I_{\text{th}} = 2.1 \times 10^{18}$ W/cm^2) was created in our experiment ($I_{\text{peak}} = 3 \times 10^{18}$ W/cm^2). Electrons released in the field at I_{th} for Kr^{18+} will gain a ponderomotive energy of approximately 220 keV. This energy is slightly less than the error bars of the maximum energy observed in the experiment, suggesting that electrons are gaining additional energy from another source.

Ionized electrons can gain additional energy from conservation of canonical momentum effects ($\vec{\text{P}}_\perp = e\vec{\text{A}}/c + \vec{\text{p}}_\perp$, where $\vec{\text{A}}$ is the vector potential, $\perp$ denotes the direction perpendicular to the laser axis, and $\vec{\text{p}}_\perp$ is the electron's momentum in this direction) [13]. Since canonical momentum P_{can} is a conserved quantity, the vector potential "component" of an electron born at rest in a field with nonzero $\vec{\text{A}}$ is converted to a translation momentum $\vec{\text{p}}_\perp$ as the electron exits the laser focus. This translational momentum is always in the direction of $\vec{\text{A}}$, resulting in electron "ejection" in the polarization direction. The ejection energy associated with P_{can} ranges from 0 for ionization when $\vec{\text{A}} = 0$ to $2\Phi_p$

for ionization when $\vec{A}$ is maximum. The trajectories of electrons released when $\vec{A} \approx 0$ will be dominated by polarization independent ponderomotive effects, resulting in azimuthally symmetric electron ejection with ejection energies of approximately Φ_p. Electrons released when $\vec{A}$ is maximum will gain a large polarization directed momentum component, resulting in azimuthally asymmetric electron ejection with ejection energies of approximately $3\Phi_p$. Obviously, the value of $\vec{A}$ at the time of ionization plays a key role in the energies and trajectories of electrons ejected from the focus. This initial value of $\vec{A}$ is determined by the ionization process and requires numerical simulations to quantitatively determine its effect on the ejected electron trajectories.

The same Monte Carlo numerical simulation used in Ref. [11] was used to model the experiment described above. In the simulation, test atoms were placed at random throughout the focal volume. A temporally and spatially Gaussian laser pulse was propagated over the atoms. Ionization of the atoms was modeled using ADK tunneling theory. The ionized electrons were released in the field with zero momentum (but nonzero P_{can} if released at nonzero values of $\vec{A}$). The freed electrons' trajectories were calculated by solving the fully relativistic Lorentz force equation of motion.

Figure 2(a) shows simulation results analogous to Fig. 1(a). The ejected electron trajectories have been projected onto a surface identical to the film surface used in the experiment to model the measurement taken with the DEF film. The ejected electron trajectories are postprocessed to model transmission through the aluminum foil used in the experiment.

The broad azimuthal peaks observed in the simulation [Fig. 2(a)] are inconsistent with the narrow peaks observed in the experiment [Fig. 1(a)]. The broad peaks in
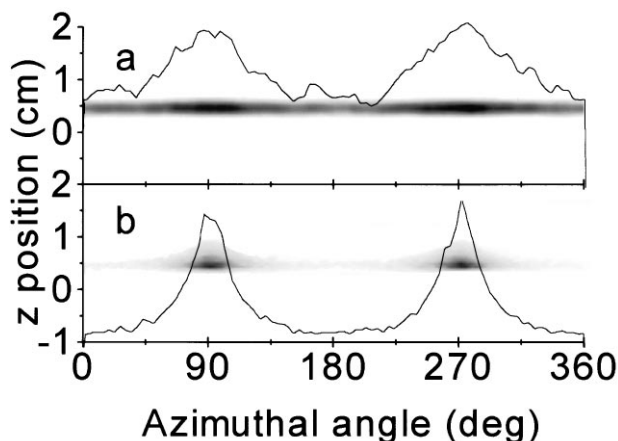

FIG. 2. Simulated ejected electron distributions from LIPA using (a) The ADK simulation and (b) the BSI simulation of the experiment. The electron distributions have been projected on a cylindrical surface identical to the experimental film position for comparison to Fig. 1. The overlayed plots are lineouts showing the azimuthal intensity distribution.

the simulation are due to the exponential field strength dependence of the ADK tunneling rate, which results in ionization only at phases very near the peaks of the rapidly oscillating electric field, i.e., when $\mathcal{E} \sim \mathcal{E}_0 \cos \Psi \sim \mathcal{E}_0$, where $\mathcal{E}_0$ contains the slowly varying temporal dependence of the field and Ψ is the phase [11]. Since the electric field and vector potential are 90° out of phase, this corresponds to a small initial $\vec{A}$ and P_{can}. The azimuthally symmetric ponderomotive acceleration therefore dominates the ejected electron trajectories, resulting in the broad peaks observed in the simulation. This simulation was used in Ref. [11], where it showed excellent agreement with LIPA experiments at lower laser intensities (7×10^{17} W/cm^2), longer pulse widths (2 ps), lower gas pressures (1 mTorr), and all other parameters similar to our experiment. The narrow peaks observed in our experiment are different from these previous results, suggesting that our higher intensity, shorter pulse width, or higher pressure has significantly altered the physics of LIPA. One possible explanation is the release of electrons with larger initial P_{can} than predicted by ADK theory (possibly due to our short pulse width or high relativistic intensity). Other possibilities include space charge deflection of the ejected electrons or a plasma instability due to our higher densities. However, space charge forces would be expected to cause a "blurring" of the electron distribution since ejected electrons will be scattered by the space charge field gradients. This blurring of the distribution was observed at pressures higher than 10 Torr but was not observed at the 1 Torr pressure used in the experiment. A plasma instability is possible although we are unaware of any instability that could result in electrons ejected in well-defined beams off the laser axis.

Under the assumption that electrons are ionized with larger initial P_{can} than predicted by ADK theory, a second simulation was performed which used a different ionization model. Since we are unaware of any ionization theory which would result in the large initial P_{can} observed in our experiment, we have modified BSI theory to allow for ionization with large initial P_{can}. The modified BSI model assumes ionization occurs at the BSI threshold intensity and imposes a $\cos^2 \Psi$ ionization probability distribution in phase; i.e., electrons are born with peak probability at the peak of the electric field and zero probability at zero electric field with a $\cos^2 \Psi$ distribution between. This empirical $\cos^2 \Psi$ probability distribution allows for ionization with substantial initial P_{can} in comparison to the exponential dependence of ADK theory since ionization can now occur at larger phase angles and correspondingly larger $\vec{A}$. Figure 2(b) shows the BSI simulation results using the experimental parameters present for the generation of Fig. 1(a). The simulation results are nearly identical to the experimental results, demonstrating that wider phase angle ionization is a strong candidate for explaining the observed azimuthal
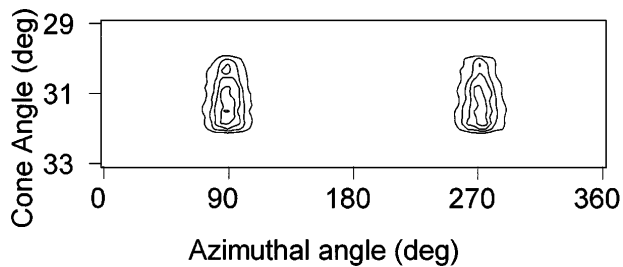
FIG. 3. The calculated ejected electron distribution for LIPA using the BSI simulation for a 2×10^{19} W/cm^2 laser focus in argon. The contours are at 20% increments relative to the maximum electron number. The average electron energy in each peak is 2.8 MeV.

asymmetry. Also apparent are electrons at smaller cone angles (the tail extending to larger z at 90° and 180°) indicating electrons with increased energy due to P_{can} effects. The tail extends to $z \approx 8$ mm corresponding to electrons with energies up to approximately 300 keV, which is within the error bars of the maximum energy observed in the experiment, 340 ± 90 keV.

The BSI simulation allows us to simulate the ionization of argon at peak intensities of 2×10^{19} W/cm^2. The angular distribution from the simulation is shown in Fig. 3. Electrons with cone angles of 30° to 32° have been selected with a simulated aperture, resulting in an average energy of 2.8 MeV and an energy spread of 300 keV (FWHM). The rms transverse emittance [20] ($\varepsilon \equiv 4\sqrt{\langle x^2 \rangle \langle x'^2 \rangle - \langle xx' \rangle^2}$) in one beam is 0.8 mm · mrad. The charge in one beam is approximately 2 pC at a background density of 1 Torr. The electron pulse length is 100 fs (FWHM) which is 4 times shorter than the laser pulse. The electron pulse compression results from rapid ionization on the laser pulse rising edge over a very small intensity range due to the highly nonlinear ionization process. This pulse compression effect scales linearly with laser pulse length. This means that a 20 fs laser pulse would generate approximately 5 fs electron pulses.

We have performed experiments and simulations which demonstrate the efficacy of LIPA as an injector for proof-of-principle laser-accelerator experiments. Electrons with up to approximately 340 keV of energy in highly directional beams have been observed in experiments. Numerical studies have found that high-energy ($E \sim 2.8$ MeV) excellent emittance beams ($\varepsilon \sim 0.8$ mm · mrad) with short bunch lengths ($\tau \sim 5$ fs) are achievable with terawatt laser systems. Laser ionization and ponderomotive acceleration can also be used as a simple single stage accelerator with very high energy capabilities. The ponderomotive energy scales linearly with intensity. Therefore, if petawatt lasers [21] can achieve near diffraction limited focal spots ($I \sim 5 \times 10^{21}$ W/cm^2), hydrogenlike argon ($I_{th} \approx 5 \times 10^{21}$ W/cm^2) could be ionized to produce ~ 1 GeV electrons.

*Permanent address: University of Rochester, Rochester, NY 14623-1299.

[1] T. Tajima and J. M. Dawson, Phys. Rev. Lett. **43**, 267 (1979); E. Esarey et al., IEEE Trans. Plasma Sci. **24**, 252 (1996).

[2] A. Modena et al., IEEE Trans. Plasma Sci. **24**, 289 (1996); C. I. Moore et al., Phys. Rev. Lett. **79**, 3909 (1997); D. Gordon et al., Phys. Rev. Lett. **80**, 2133 (1998); A. Ogata et al., Bull. Am. Phys. Soc. **42**, 1967 (1997).

[3] C. G. Durfee III et al., Phys. Rev. Lett. **71**, 2409 (1993); Y. Ehrlich et al., Phys. Rev. Lett. **77**, 4186 (1996); R. Wagner et al., Phys. Rev. Lett. **78**, 3125 (1997); K. Krushelnick et al., Phys. Rev. Lett. **78**, 4047 (1997); S.-Y. Chen et al., Phys. Rev. Lett. **80**, 2610 (1998); C. Clayton et al., Phys. Rev. Lett. **81**, 100 (1998).

[4] Y. Kitagawa et al., Phys. Rev. Lett. **68**, 48 (1992); C. E. Clayton et al., Phys. Rev. Lett. **70**, 37 (1993); N. A. Ebrahim, J. Appl. Phys. **76**, 7645 (1994); F. Amiranoff et al., Phys. Rev. Lett. **74**, 5220 (1995).

[5] G. Malka et al., Phys. Rev. Lett. **78**, 3314 (1997).

[6] W. D. Kimura et al., Phys. Rev. Lett. **74**, 546 (1995); A. van Steenbergen et al., Phys. Rev. Lett. **77**, 2690 (1996).

[7] J. R. Marquès et al., Phys. Rev. Lett. **76**, 3566 (1996); C. W. Siders et al., Phys. Rev. Lett. **76**, 3570 (1996).

[8] D. Umstadter et al., Phys. Rev. Lett. **76**, 2073 (1996).

[9] E. Esarey et al., Phys. Rev. Lett. **79**, 2682 (1997).

[10] C. I. Moore et al., Phys. Rev. Lett. **74**, 2439 (1995); S. J. McNaught et al., Phys. Rev. Lett. **78**, 626 (1997).

[11] S. J. McNaught et al., Phys. Rev. A **58**, 1399 (1998).

[12] L. S. Brown and T. W. B. Kibble, Phys. Rev. **133**, A705 (1964); B. Quesnel and P. Mora, Phys. Rev. E **58**, 3719 (1998).

[13] P. B. Corkum et al., Phys. Rev. Lett. **62**, 1259 (1989); W. B. Mori and T. Katsouleas, Phys. Rev. Lett. **69**, 3495 (1992).

[14] P. Monot et al., J. Opt. Soc. Am. B **9**, 1579 (1992); W. P. Leemans et al., Phys. Rev. A **46**, 1091 (1992); D. Umstadter and X. Liu, in *Advanced Accelerator Concepts,* edited by J. S. Wurtele, AIP Conf. Proc. No. 279 (AIP, New York, 1993), p. 450; P. Sprangle et al., Phys. Rev. Lett. **79**, 1046 (1997).

[15] *American Institute of Physics Handbook,* edited by Dwight E. Gray (McGraw-Hill, New York, 1982), 3rd ed.

[16] J. N. Bardsley et al., Phys. Rev. A **40**, 3823 (1989); H. R. Reiss, J. Opt. Soc. Am. B **7**, 574 (1990); P. B. Corkum et al., in *Atoms in Intense Fields,* edited by M. Gavrila (Academic Press, Boston, 1992).

[17] L. D. Landau and E. M. Lifshitz, *Quantum Mechanics* (Pergamon, New York, 1965).

[18] M. V. Ammosov et al., Sov. Phys. JETP **64**, 1191 (1986).

[19] S. Augst et al., Phys. Rev. Lett. **63**, 2212 (1989).

[20] J. D. Lawson, *The Physics of Charged-particle Beams* (Clarendon Press, Oxford, 1977), p. 199.

[21] B. C. Stuart et al., Opt. Lett. **22**, 242 (1997).